JVI Journals.ASM.org

Identification of Common Mechanisms by Which Human and Mouse Cytomegalovirus Seven-Transmembrane Receptor Homologues Contribute to *In Vivo* Phenotypes in a Mouse Model

Helen E. Farrell,[a] Alexander M. Abraham,[a] Rhonda D. Cardin,[b] Ann-Sofie Mølleskov-Jensen,[c] Mette M. Rosenkilde,[c] Nicholas Davis-Poynter[a]

The University of Queensland, Clinical Medical Virology Centre & Royal Children's Hospital, Sir Albert Sakzewski Virus Research Centre, Brisbane, Queensland, Australia[a]; Division of Infectious Diseases, Cincinnati Children's Hospital Medical Center, Cincinnati, Ohio, USA[b]; Department of Neuroscience and Pharmacology, Faculty of Health and Medical Sciences, University of Copenhagen, Copenhagen, Denmark[c]

The mouse cytomegalovirus chemokine receptor homologue (CKR) M33 is required for salivary gland tropism and efficient reactivation from latency, phenotypes partially rescued by the human cytomegalovirus CKR US28. Herein, we demonstrate that complementation of salivary gland tropism is mediated predominantly by G protein-dependent signaling conserved with that of M33; in contrast, both G protein-dependent and -independent pathways contribute to the latency phenotypes. A novel M33-dependent replication phenotype in cultured bone marrow macrophages is also described.

All beta- and gammaherpesviruses express one or more 7-transmembrane receptor homologues (7TMR), several of which have been implicated in viral pathogenesis and are thereby regarded as potential therapeutic targets (1). Human cytomegalovirus (HCMV) encodes four 7TMRs: UL33, UL78 (conserved in all betaherpesviruses), and US27 and US28, which are encoded by tandem genes (restricted to primate CMV). Of these, US28, a CC chemokine receptor homologue (CKR) has been the most thoroughly characterized. Unlike most cellular CKR, US28 exhibits promiscuous binding of CC chemokines and the membrane-tethered CX3CL1 chemokine fractalkine. As these chemokines elicit chemotactic responses of monocytes and vascular endothelial cells, US28 has been implicated in virus dissemination. US28 has been shown to signal constitutively via Gαq (2) and the mitogen-activated protein kinase (MAPK) pathways (3–5) and invoke activation of transcription factors, including NF-κB, CREB, NFAT, and SRE (2–4, 6, 7). Potential consequences of the diverse signaling cascade elicited by US28 include modulation of the expression of host genes involved in pathogenesis, enhancement of replication in particular cell types, and triggering reactivation from latency (8, 9). Similar to several other viral CKRs, US28 is rapidly and constitutively endocytosed, providing a mechanism for both regulation of G protein-dependent signaling and initiation of G protein-independent signaling (3, 5, 10, 11).

Previous characterization of N- and C-terminal US28 mutations demonstrated the importance of particular US28 domains in receptor signaling and endocytosis. The US28 C-tail is necessary and sufficient to confer efficient endocytosis to US28 and heterologous CKR (3). C-terminal truncations of US28 (ΔC36, ΔC40, and ΔC54) have revealed modulatory effects on either classical G protein-mediated phospholipase C-β (PLC-β) signaling, engagement of the p38 MAP kinase pathway, or activation of NF-κB and CREB transcription factors (3, 5, 12). Mutation of the highly conserved arginine within the transmembrane III DRY motif abolished constitutive G protein-mediated signaling, but the mutant protein retained constitutive endocytosis (3).

Models for the *in vivo* function of HCMV-encoded CKRs have utilized mouse and rat CMVs (MCMV and RCMV, respectively). We previously established that the MCMV homologue of HCMV UL33 (M33) is important for salivary gland tropism and establishment of and/or reactivation from latency (13–15). Mutagenesis of M33 demonstrated that while salivary gland tropism was partly preserved in the absence of the M33 C tail, it was highly dependent on M33 G protein coupling (14). In contrast, MCMV latency and/or reactivation was substantially reduced with mutation of either the DRY motif or the M33 C tail, suggesting that both G protein-dependent and -independent mechanisms are important for the latency phenotype (16; H. E. Farrell and N. Davis-Poynter, unpublished observations). Notably, we demonstrated that wild-type (wt) HCMV US28 can partially substitute for the role of M33 *in vivo*, thus providing the first surrogate animal model to probe the mechanisms of action of US28 (16).

Given the importance of the M33 TMIII DRY and C-tail motifs *in vivo*, we investigated the roles of analogous motifs of US28 on M33 complementation *in vivo*. US28 mutants comprised either a point mutation disrupting the DRY motif (US28R129Q), a truncation of the C terminus (US28ΔC54), or a dual R129Q/ΔC54 mutant (US28RQ/ΔC54). A US28 mutant with a deletion of N-terminal residues (US28ΔN[2-16]), which disrupted fractalkine binding (17, 18), was included as a control in some studies.

Expression constructs were tagged with hemagglutinin (HA) at the N terminus; recombinant viruses derived from the wild-type (wt) MCMV strain K181 (Perth) are described in Table 1. Statistical analyses were conducted using GraphPad Prism v 5.0.

Cell surface expression and endocytosis in transfected cells were measured using a cell-based enzyme-linked immunosorbent assay (ELISA) and antibody feeding/immunofluorescence, respectively, using methods similar to those described previously (19, 20). At steady state, US28ΔC54 and US28RQ/ΔC54 were expressed mostly at the cell surface, in contrast to wt US28, US28R129Q, and US28ΔN[2-16] (Fig. 1A). Higher levels of cell

Received 10 December 2012 **Accepted** 17 January 2013
Published ahead of print 23 January 2013
Address correspondence to Nicholas Davis-Poynter, n.davispoynter@uq.edu.au.

doi:10.1128/JVI.03406-12

TABLE 1 Descriptions of recombinant viruses

Virus	Description of altered MCMV M33 locus	Source or reference
ΔM33/Z[a]	M33 null via *lacZ* insertion	KΔ33BT2 (15)
ΔM33/STOP	M33 null via premature stop codon	16
M33R131Q	M33 point mutant defective for G protein-coupled signaling	14
wt US28	Replaced by wild-type US28 (HCMV strain AD169)	16
US28R129Q	Replaced by US28 defective for G protein-coupled signaling	Recombination plasmid (JX183618[b])
US28ΔC54	Replaced by US28 deleted of C-terminal 54 amino acids	Recombination plasmid (JX183619[b])
US28RQ/ΔC54	Replaced by US28 with both the R129Q point mutation and ΔC54 truncation	Recombination plasmid (JX183621[b])

[a] ΔM33/Z was the parent virus for all other recombinants.
[b] GenBank accession number of the plasmid used to generate the virus recombinant, according to published methods (14–16).

surface expression of both US28ΔC54 mutants correlated with their decreased endocytosis (Fig. 1B), consistent with previous reports of the US28 C tail directing endocytosis. Nevertheless, comparison between US28ΔC54 and CCR5 (cell surface-retained control) suggests that a low level of endocytosis of US28 occurred in the absence of the C tail. In mouse embryonic fibroblasts (MEF) infected with either untagged wt US28 or mutant US28 recombinant MCMV, ^{125}I-CX$_3$CL1 radioligand binding experiments, using methods similar to those described previously (16), demonstrated high-affinity binding by all viruses (Fig. 1C), except the negative control US28ΔN[2-16], which was disrupted for fractalkine binding (17). Endocytosis experiments using ^{125}I-CX$_3$CL1 with MCMV-infected MEF (24 h postinfection [p.i.]) confirmed that wt US28 and US28R129Q were rapidly endocytosed, in contrast to the US28ΔC54 mutants (data not shown).

G protein-coupled signaling (PLC-β activation) of US28 mutants in transfected COS7 and MCMV-infected cells was compared with that of wt US28. In transfected and infected cells (Fig. 2A and B, respectively), inositol turnover was abolished, as expected, for each of the US28R129Q mutants (Fig. 2). US28ΔC54 had reduced signaling and thus exhibited an effect similar to that of the C-terminal truncation (ΔC38) of M33 (14); this contrasts with a previous report describing increased inositol turnover for a US28ΔC54 mutant in transfected cells (5). Consistent with previous studies, fractalkine proved to be an inverse agonist for wt US28, which was converted to agonism in US28ΔC54. Fractalkine did not affect signaling of US28R129Q, US28RQ/ΔC54, or US28ΔN[2-16], confirming that the effects were G protein dependent and initiated by binding of fractalkine to US28. These results demonstrate that PLC-β signaling, chemokine binding, and endocytic properties of wt US28 and the US28 mutants used in this study were consistent with those in previous reports of transfected

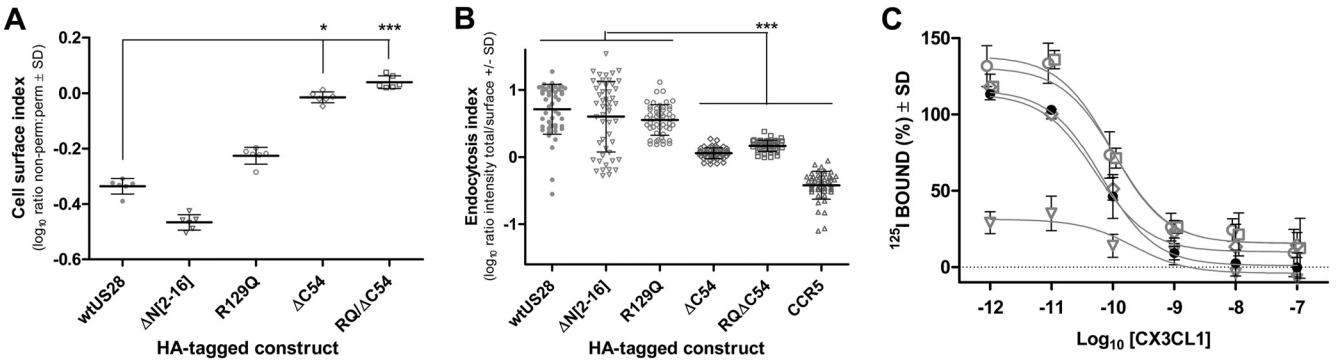

FIG 1 (A) Expression levels of HA-tagged US28 constructs detected by ELISA. COS-7 cells in 6-well dishes were transfected with 4 μg of the indicated HA-tagged US28 constructs or the pcDNA3 vector control using Lipofectamine 2000 (Invitrogen, Australia). At 6 h posttransfection, cells were trypsinized and seeded into replicate 96-well trays (six wells per construct per plate). The detection of the HA-tagged constructs in cells permeabilized with Triton X-100 and nonpermeabilized replicate cells was performed 24 h later as described previously (19). Receptor levels were measured as optical density (OD) readings at 450 nm and corrected for background via subtraction of mean control values (perm. or non-perm.). Data are presented as a cell surface index, i.e., the $\log_{10}$ ratio of the cell surface (nonpermeabilized) to total (permeabilized) OD values. Bars indicate means and standard deviations (SD) ($n = 6$). Asterisks indicate significant differences between the wt and mutated US28 constructs (Kruskal-Wallis with Dunn's posttest, *, $P < 0.05$; ***, $P < 0.001$). (B) Quantitative assessment of endocytosis for wt US28 and US28 mutants. HeLa cells transfected with 4 μg of the indicated HA-tagged constructs using Lipofectamine 2000 were labeled with rabbit anti-HA (ab9110, 1:500; Abcam, Cambridge, United Kingdom) at 37°C for 1 h and then "chased" in the absence of antibody for a further 20 min. Endocytosis was stopped by incubating cells at 4°C and cell surface-retained receptors labeled with Alexa Fluor 594 (AF^{594}) goat anti-rabbit IgG (1:1,000; A11037; Molecular Probes, Invitrogen, Australia) for 1 h at 4°C. The cells were fixed with 3% paraformaldehyde, permeabilized with 0.2% Triton X-100, and incubated with AF^{488} goat anti-rabbit IgG (A11034, 1:1,000; Molecular Probes, Invitrogen, Australia) for 1 h at room temperature. Images from random fields captured at a magnification of ×40 were converted to grayscale; the AF^{488} and AF^{594} channels were overlaid, and the ratio of AF^{488} (total) to AF^{594} (surface) staining of individual cells was determined using NIH ImageJ (http://rsb.info.nih.gov/ij/). The $\log_{10}$ ratio provides an endocytosis index; this ratio increases as the proportion of endocytosed receptors increases. Data are plotted for individual cells, with bars indicating means and SD (50 cells). Asterisks indicate significant differences between the wt and other constructs (Kruskal-Wallis with Dunn's posttest, ***, $P < 0.001$). (C) Surface expression of wt US28 and US28 mutants determined by whole-cell binding of the chemokine ligand ^{125}I-CX3CL1 (fractalkine) as described previously (27). Whole-cell homologous competition binding was performed in MEF infected (MOI = 3) with either wt US28 (filled circles), US28ΔN[2-16] (open triangles), US28R129Q (open circles), US28ΔC54 (open diamonds), or US28RQ/ΔC54 (open squares). At 24 h p.i., cells were labeled with ^{125}I-CX3CL1 (fractalkine) and incubated with increasing amounts of cold CX3CL1 as indicated. Data are means ± SD from two experiments performed in triplicate.

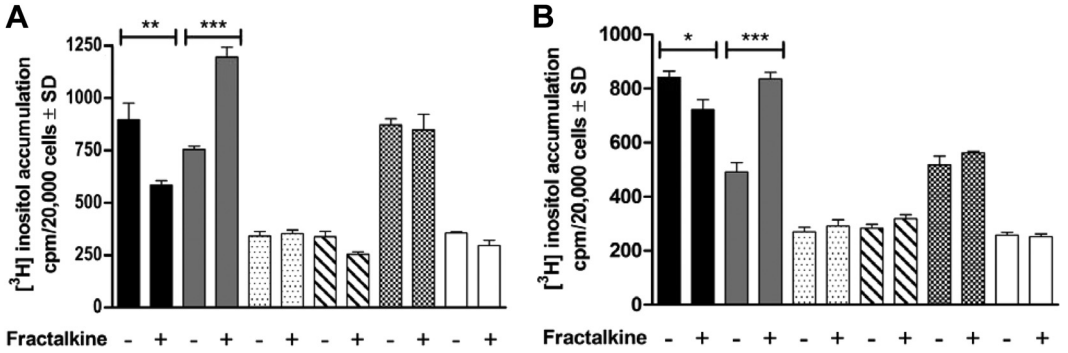

FIG 2 Inositol phosphate turnover in transfected or MCMV-infected cells. (A) COS7 cells transfected 24 h previously with constructs expressing either wt US28 (black), US28ΔC54 (gray), US28R129Q (stippled), US28RQ/ΔC54 (striped), US28ΔN[2–16] (checked), or pcDNA3 (white). (B) MEF infected (MOI = 3) 24 h previously with MCMV recombinants expressing either wt or mutated US28 (shading as in panel A) or an M33-null mutant (white). In both panels, cells were incubated in the presence or absence of 10 nM human recombinant CX3CL1, prior to determination of accumulation of phosphorylated [^{3}H]inositol according to methods described previously (28). Data are presented as means ± SD from 2 experiments performed in triplicate; asterisks indicate significant difference between the responses with and without fractalkine (Student's *t* test; *, $P < 0.05$; **, $P < 0.01$; ***, $P < 0.001$).

or HCMV-infected cells (3, 5, 12, 18) and thus were authentically expressed by recombinant MCMV.

US28 has the potential to induce signaling effectors, such as the mitogen-activated protein kinases (MAPK), via both G protein-dependent and -independent mechanisms. Endocytosed 7TMRs have been shown to scaffold various key contributors to the MAPK signaling cascade, including ERK1/2, p38, and c-Jun N-terminal kinase (JNK), a process involving phosphorylation of 7TMR C-tail residues (21). In transfected COS7 cells, US28 induces p38 MAPK activity (3–5), which is diminished in a ΔC54 tail mutant (5). In addition, US28 and M33-mediated signaling is sensitive to p38 but not ERK1/2 kinase inhibitors (3, 22), although subsequent studies have shown ERK1/2 to be induced by fractalkine binding in US28-transduced murine fibroblasts (23). Thus, we determined the impact of the DRY and C-tail US28 mutations on activation of these MAPK. Using Western blotting with phosphospecific antibodies (Cell Signaling Technology), wt US28 was shown to engage all three MAPK in transfected HEK cells (Fig. 3). An approximate 2-fold reduction of p38 MAPK activity ($P < 0.05$) was observed in the dual RQ/ΔC54 US28 mutant, whereas the single mutants were not significantly different from the wild type, consistent with previous studies showing that p38 MAPK is induced by both G protein-dependent and -independent mechanisms (13, 22, 25). In contrast, p-ERK1/2 and p-JNK MAPK induction was diminished ($P < 0.001$ and $P < 0.01$, respectively) only in the absence of G protein coupling (mutants R129Q and RQ/ΔC54), suggesting that the US28 C tail was dispensable for their induction. None of the mutations, including RQ/ΔC54, reduced MAPK activation to control levels (pcDNA3). Given that US28ΔC54 and RQ/ΔC54 exhibited low-level endocytosis (compared with CCR5), these mutants may retain the capacity to initiate MAPK or additional signaling pathways, via scaffold interactions, despite the absence of the C tail.

US28 constitutively activates multiple transcription factors, in-

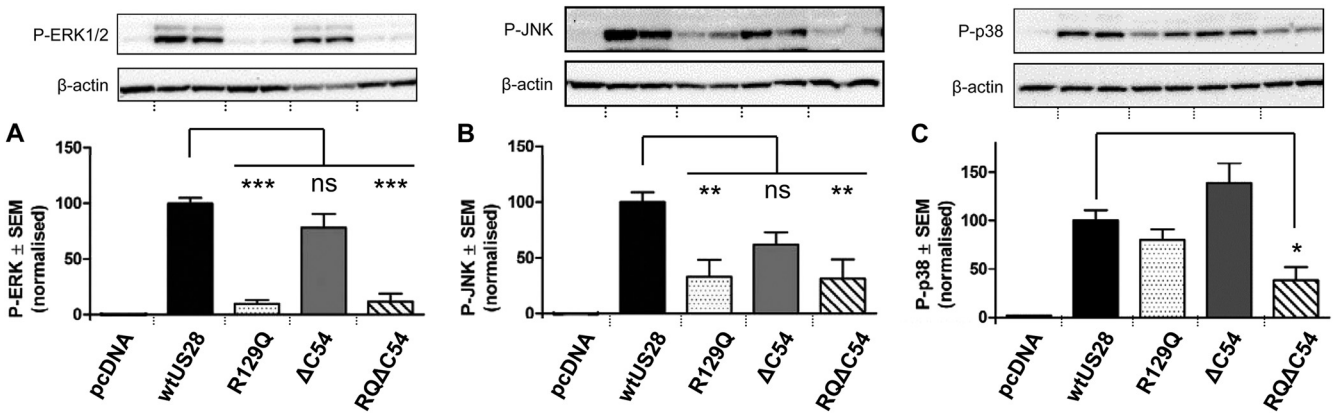

FIG 3 HEK293 cells were transfected with 20 μg of the indicated HA-tagged US28 constructs or the pcDNA3 vector using calcium chloride precipitation. At 48 h after transfection, the cells were lysed on ice using radioimmunoprecipitation assay (RIPA) lysis buffer (Millipore). Samples were denatured at 92°C for 5 min and run on a 10% bis-Tris gel (Invitrogen) at 130 V for 1.5 h. The gel was blotted onto polyvinylidene difluoride (PVDF) membranes for 1.5 h and incubated with phosphospecific antibodies (Cell Signaling) against ERK (A) and JNK (B) simultaneously or p38 (C) overnight at 4°C. After incubation with horseradish peroxidase (HRP)-conjugated secondary antibodies, the membranes were developed using Immobilon Western chemiluminescent (Millipore) and quantified using AlphaView software; blots were stripped and reprobed for β-actin as a loading control. For each blot, background signal (pcDNA3) was subtracted and results were expressed relative to the mean signal for wt US28 (100%). Results are expressed as means ± standard errors of the means (SEM) from five independent experiments, each performed with duplicate samples. Representative blots are shown above the quantification graphs in each case. Asterisks denote significant differences between wt US28 and US28 mutants (analysis of variance [ANOVA] with Bonferroni posttest; *, $P < 0.05$; **, $P < 0.01$; ***, $P < 0.001$).

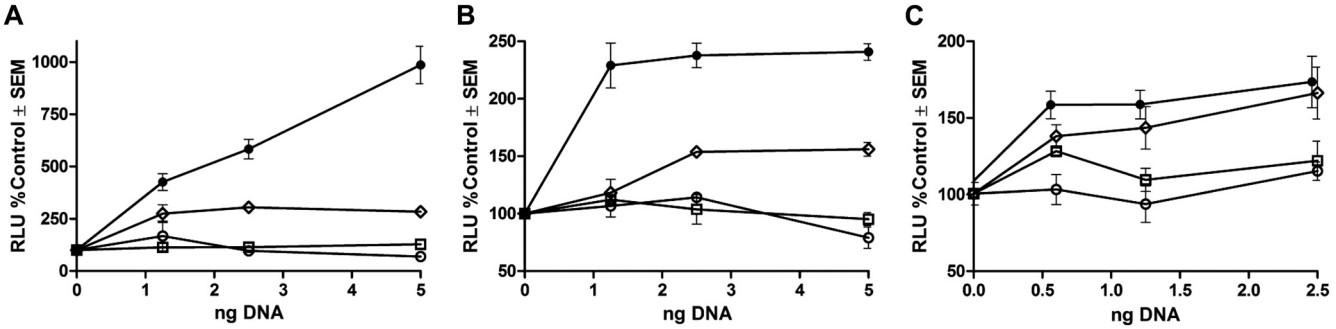

FIG 4 Induction of CREB-driven (A), NF-κB-driven (B), and NFAT-driven (C) luciferase expression in HEK cells transfected with either 50 ng of CREB-luciferase DNA (A), 50 ng NF-κB-luciferase DNA (B), or 50 ng NFAT-luciferase (C) together with increasing concentrations of either wt US28 (●), US28ΔC54 (◇), US28R129Q (○), or US28RQ/ΔC54 (□) expression plasmids. Experiments were performed according to previously reported methods (14). Baseline signaling measurements of HEK cells transfected with equivalent amounts of the pcDNA3 expression vector were set at 100%. Data are means ± SEM from two experiments performed in quadruplicate.

cluding CREB, NF-κβ, and, to a lesser extent, NFAT (2, 4, 24). G protein coupling appears to be the predominant mechanism, since the DRY motif mutants (R129Q and RQ/ΔC54) were deficient (Fig. 4). Partial reductions in activation exhibited by US28ΔC54 are consistent with the observed reduction in PLC-β signaling (Fig. 2), although potential G protein-independent mechanisms of modulation of these transcription factors cannot be ruled out. Similar to US28, significant reduction in CREB activation was observed previously with the M33 DRY (R131Q) and C-tail truncation (ΔC38) mutants, where the latter showed reduced but not abolished Gαq protein-dependent signaling (14).

All of the US28 recombinants replicated to wt MCMV levels in MEF (data not shown), consistent with our previous observations of M33-null mutants (15). However, recent studies in our laboratory identified an *in vitro* phenotype for M33 in primary bone marrow macrophage (BMM) cultures. Thus, M33-null mutants were significantly attenuated for multistep growth in BMM (Fig. 5A). Attenuation was not observed following infection with a high multiplicity of infection (MOI), suggesting a defect(s) in cell-cell spread of the virus (data not shown). Notably, wt US28 compensated for the loss of M33 (Fig. 5B), but this compensation did not appear to be associated with aforementioned signaling pathways, since M33 and US28 TMIII DRY signaling knockout mutants (M33R131Q and US28R129Q), C-tail truncation mutants (M33ΔC38 and US28ΔC54), and the US28 dual mutant (RQ/ΔC54) each replicated to wt M33 levels (Fig. 5). While the mechanism of attenuation is currently unknown, these results suggest that M33 and US28 possess mechanisms independent of the G protein-mediated signaling profiles examined here that can compensate for the replication fitness afforded by wt M33 in BMM.

The US28 mutants were analyzed *in vivo* with respect to replication during acute infection, tropism to the salivary glands, and *ex vivo* reactivation of latently infected splenic explants using methods described previously (13, 16). Each of the US28 virus mutants replicated in the spleen and liver to wt MCMV levels (Fig. 6A), supporting our previous studies that the M33 locus is dispensable during acute infection (13–16). In the salivary glands, the two US28R129Q mutants were significantly attenuated compared with wt US28 (Fig. 6B), correlating with their reduced Gαq PLC-β signaling and consistent with our previous demonstration that M33 requires G protein-mediated signaling for this phenotype (14). In addition, our results demonstrate that the C terminus of US28 is dispensable for this phenotype, providing further evidence, based on the US28ΔC54 signaling profile, that US28-me-

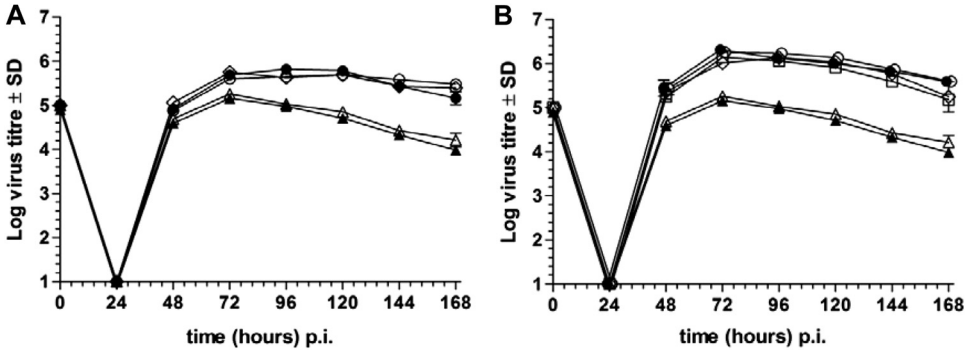

FIG 5 Multistep growth analysis of M33 MCMV recombinants (A) and US28 recombinants (B) in primary BMM cultures from adult C57BL/6 mice. BMM were harvested from femurs and tibias of mice and cultured in the presence of human recombinant colony-stimulating factor 1 (CSF-1; 10^4 U/ml; a kind gift from M. Sweet, University of Queensland) for 5 to 9 days. BMM were infected at an MOI of 10 (relative to MEF; corresponds to an MOI of approximately 0.1 for BMM); supernatants were taken at the indicated times and assayed for infectious virus by plaque assay on MEF. (A) wt M33 (●), M33R131Q (○), M33ΔC38 (◇), and M33-null mutants (*lacZ* insertion [▲] and M33 premature stop [△]); (B) wt US28 (●), US28ΔC54 (◇), US28R129Q (○), US28RQ/ΔC54 (□) and M33-null mutants (*lacZ* insertion [▲] and M33 premature stop [△]). Data are mean titers ($\log_{10}$ PFU/ml) ± SD from two experiments performed in triplicate. The origin of the *y* axis is adjusted to reflect the lower limit of virus detection.

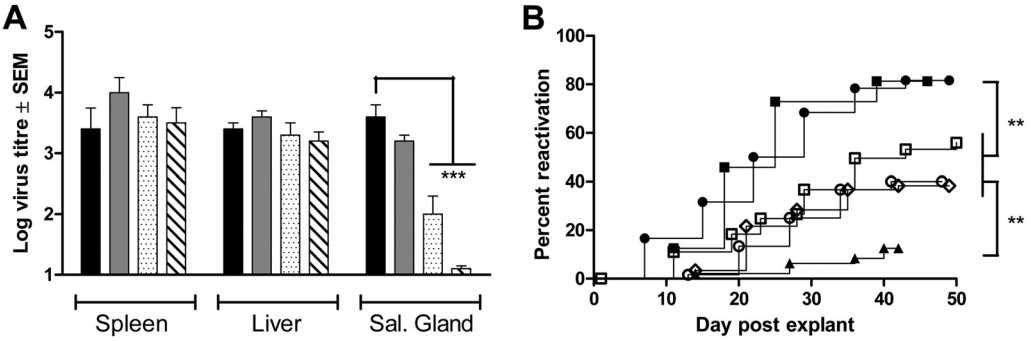

FIG 6 (A) Replication of recombinant MCMV expressing wild-type or mutated US28 in BALB/c mice. Six-week-old mice were inoculated i.p. with 2×10^6 PFU of either wt US28 recombinant MCMV (black) or the following US28 mutant MCMVs: US28ΔC54 (gray), US28R129Q (stippled), or US28RQ/ΔC54 (striped). Organs ($n = 4$) were harvested at 4 days p.i. (spleen and liver) or 17 days p.i. (salivary gland). Virus titers of homogenized organs ($\log_{10}$ PFU/organ) were quantified on MEF by plaque assay. The origin of the *y* axis is adjusted to reflect the lower limit of virus detection. Comparisons between wt US28 and US28 mutant groups were made using ANOVA with a Bonferroni posttest (***, $P < 0.001$). (B) Cumulative reactivation curves of spleen explant cultures taken from latently infected adult BALB/c mice. Spleens (10 to 20 per group) were harvested 12 weeks following i.p. infection of 10^5 PFU of either wt K181 (■), wt US28 (●), US28ΔC54 (◇), US28R129Q (○), US28RQ/ΔC54 (□), or M33R131Q (▲). Each spleen was finely dissected and distributed among 6 wells of a 24-well culture plate (i.e., 60 to 120 cultures in total). Supernatants (80 μl) were harvested twice during the first week and once per week for a period of 6 to 8 weeks and assayed for infectious virus on MEF by centrifugal enhancement. Cultures that were positive within the first 7 days (≤3% of total cultures) were likely to represent persistent shedding rather than a reactivation event and were excluded from the analysis. Comparisons of the proportion of reactivated to nonreactivated cultures were made using Fisher's exact test (**, $P < 0.01$).

diated tropism to the salivary gland in the context of MCMV infection is highly G protein dependent (14). Nevertheless, the detection of the US28R129Q mutant at low levels in the salivary gland and the observation that the phenotype was further attenuated for the dual RQ/ΔC54 mutant suggests that additional mechanisms, such as MAPK signaling, may contribute.

Previously, we found that a M33-null, G protein-coupling-deficient mutant (M33R131Q) and a M33 C-tail mutant had a severely diminished capacity to reactivate from splenic explants, a phenotype that could be fully compensated by wt US28 (13, 16). Characterization of the US28 mutants (Fig. 6) similarly demonstrated that both DRY motif and C-tail mutants had reduced reactivation rates.

While the mechanisms by which M33 and US28 promote reactivation from latency are unknown, it is tempting to suggest that induction of transcription factors by these viral 7TMR participate in this process. Like HCMV, enhancer regions regulating expression of important MCMV transactivator proteins contain CRE and NF-κB sites that, upon binding with the cognate ligand, transactivate viral major immediate-early genes that lead to "desilencing" of the latent genome. However, it is also important to note that none of the US28 mutations reduced reactivation to the level of M33(R131Q), demonstrating that mechanisms other than those targeted by the US28 R129Q and ΔC54 mutations can partially compensate for the loss of G protein-mediated pathways. Given that the US28 mutants retained MAPK induction, it is tempting to suggest that they may contribute to the reactivation detected by the US28 mutants. Indeed, as CMV reactivation is frequently associated with host cell differentiation and inflammation—processes that commonly engage one or more of the MAPK—it is possible that US28-mediated induction of these mediators may contribute a trigger for CMV in the maintenance and/or reactivation of latency. In this regard, treatment of latently infected cells with inhibitors of MAPK has been shown to block the production of interleukin 6 (IL-6) by dendritic cells that is a significant prerequisite for CMV reactivation (25, 26). Further studies using additional US28 MCMV mutants that differ in their profiles of MAPK induction are in progress to determine the significance of US28-mediated MAPK induction the maintenance and reactivation from latency. In summary, the MCMV model provides a useful quantitative readout to probe the biological contributions of constitutive US28 signaling. Our results demonstrate that common 7TMR G protein-dependent mechanisms are major contributors to both US28 and M33 phenotypes in salivary gland tropism and latency. With respect to latency, our data also suggest a role for G protein-independent mechanisms in this phenotype, for which the MAPK may play a role. Finally, we provide evidence that M33 is required for efficient replication in differentiated BMM, a property that could be compensated for by US28 via mechanisms not linked to G protein-dependent signaling and which may impact dissemination of virus infection to sites such as the salivary gland. Future studies will be directed at identifying specific cellular signaling pathways that have the most impact upon phenotypes dependent upon US28 and M33, using a combination of comparative profiling (between mutants with differing phenotypes) and selective ablation of host cell signaling.

ACKNOWLEDGMENTS

This work was supported by grants from the NHMRC (project grant 631401, N.D.-P. and H.F.) and the NIH (RO1 grant AI087683, R.C. and H.F.).

REFERENCES

1. **Rosenkilde MM, Kledal TN.** 2006. Targeting herpesvirus reliance of the chemokine system. Curr. Drug Targets **7**:103–118.
2. **Casarosa P, Bakker RA, Verzijl D, Navis M, Timmerman H, Leurs R, Smit MJ.** 2001. Constitutive signaling of the human cytomegalovirus-encoded chemokine receptor US28. J. Biol. Chem. **276**:1133–1137.
3. **Waldhoer M, Casarosa P, Rosenkilde MM, Smit MJ, Leurs R, Whistler JL, Schwartz TW.** 2003. The carboxyl terminus of human cytomegalovirus-encoded 7 transmembrane receptor US28 camouflages agonism by mediating constitutive endocytosis. J. Biol. Chem. **278**:19473–19482.
4. **McLean KA, Holst PJ, Martini L, Schwartz TW, Rosenkilde MM.** 2004. Similar activation of signal transduction pathways by the herpesvirus-encoded chemokine receptors US28 and ORF74. Virology **325**:241–251.
5. **Miller WE, Houtz DA, Nelson CD, Kolattukudy PE, Lefkowitz RJ.**

2003. G protein-coupled receptor (GPCR) kinase phosphorylation and beta-arrestin recruitment regulate the constitutive signaling activity of the human cytomegalovirus US28 GPCR. J. Biol. Chem. **278**:21663–21671.
6. **Moepps B, Tulone C, Kern C, Minisini R, Michels G, Vatter P, Wieland T, Gierschik P.** 2008. Constitutive serum response factor activation by the viral chemokine receptor homologue pUS28 is differentially regulated by Galpha(q/11) and Galpha(16). Cell Signal. **20**:1528–1537.
7. **Wen DQ, Zhang YY, Lv LP, Zhou XP, Yan F, Ma P, Xu JB.** 2009. Human cytomegalovirus-encoded chemokine receptor homolog US28 stimulates the major immediate early gene promoter/enhancer via the induction of CREB. J. Recept. Signal Transduct. Res. **29**:266–273.
8. **Rosenkilde MM, Smit MJ, Waldhoer M.** 2008. Structure, function and physiological consequences of virally encoded chemokine seven transmembrane receptors. Br. J. Pharmacol. **153**(Suppl. 1):S154–S166.
9. **Vischer HF, Leurs R, Smit MJ.** 2006. HCMV-encoded G protein-coupled receptors as constitutively active modulators of cellular signaling networks. Trends Pharmacol. Sci. **27**:56–63.
10. **Fraile-Ramos A, Kledal TN, Pelchen-Matthews A, Bowers K, Schwartz TW, Marsh M.** 2001. The human cytomegalovirus US28 protein is located in endocytic vesicles and undergoes constitutive endocytosis and recycling. Mol. Biol. Cell **12**:1737–1749.
11. **Mokros T, Rehm A, Droese J, Oppermann M, Lipp M, Hopken UE.** 2002. Surface expression and endocytosis of the human cytomegalovirus-encoded chemokine receptor US28 is regulated by agonist-independent phosphorylation. J. Biol. Chem. **277**:45122–45128.
12. **Stropes MP, Schneider OD, Zagorski WA, Miller JL, Miller WE.** 2009. The carboxy-terminal tail of human cytomegalovirus (HCMV) US28 regulates both chemokine-independent and chemokine-dependent signaling in HCMV-infected cells. J. Virol. **83**:10016–10027.
13. **Cardin RD, Schaefer GC, Allen JR, Davis-Poynter NJ, Farrell HE.** 2009. The M33 chemokine receptor homolog of murine cytomegalovirus exhibits a differential tissue-specific role during in vivo replication and latency. J. Virol. **83**:7590–7601.
14. **Case R, Sharp E, Benned-Jensen T, Rosenkilde MM, Davis-Poynter N, Farrell HE.** 2008. Functional analysis of the murine cytomegalovirus chemokine receptor homologue M33: ablation of constitutive signaling is associated with an attenuated phenotype in vivo. J. Virol. **82**:1884–1898.
15. **Davis-Poynter NJ, Lynch DM, Vally H, Shellam GR, Rawlinson WD, Barrell BG, Farrell HE.** 1997. Identification and characterization of a G protein-coupled receptor homolog encoded by murine cytomegalovirus. J. Virol. **71**:1521–1529.
16. **Farrell HE, Abraham AM, Cardin RD, Sparre-Ulrich AH, Rosenkilde MM, Spiess K, Jensen TH, Kledal TN, Davis-Poynter N.** 2011. Partial functional complementation between human and mouse cytomegalovirus chemokine receptor homologues. J. Virol. **85**:6091–6095.
17. **Casarosa P, Waldhoer M, LiWang PJ, Vischer HF, Kledal T, Timmerman H, Schwartz TW, Smit MJ, Leurs R.** 2005. CC and CX3C chemokines differentially interact with the N terminus of the human cytomegalovirus-encoded US28 receptor. J. Biol. Chem. **280**:3275–3285.
18. **Stropes MP, Miller WE.** 2008. Functional analysis of human cytomegalovirus pUS28 mutants in infected cells. J. Gen. Virol. **89**:97–105.
19. **Tschische P, Tadagaki K, Kamal M, Jockers R, Waldhoer M.** 2011. Heteromerization of human cytomegalovirus encoded chemokine receptors. Biochem. Pharmacol. **82**:610–619.
20. **Sharp EL, Davis-Poynter NJ, Farrell HE.** 2009. Analysis of the subcellular trafficking properties of murine cytomegalovirus M78, a 7 transmembrane receptor homologue. J. Gen. Virol. **90**:59–68.
21. **Shukla AK, Xiao KH, Lefkowitz RJ.** 2011. Emerging paradigms of beta-arrestin-dependent seven transmembrane receptor signaling. Trends Biochem. Sci. **36**:457–469.
22. **Smit MJ, Verzijl D, Casarosa P, Navis M, Timmerman H, Leurs R.** 2002. Kaposi's sarcoma-associated herpesvirus-encoded G protein-coupled receptor ORF74 constitutively activates p44/p42 MAPK and Akt via G(i) and phospholipase C-dependent signaling pathways. J. Virol. **76**:1744–1752.
23. **Vomaske J, Melnychuk RM, Smith PP, Powell J, Hall L, DeFilippis V, Fruh K, Smit M, Schlaepfer DD, Nelson JA, Streblow DN.** 2009. Differential ligand binding to a human cytomegalovirus chemokine receptor determines cell type-specific motility. PLoS Pathog. **5**:e1000304. doi:10.1371/journal.ppat.1000304.
24. **Waldhoer M, Kledal TN, Farrell H, Schwartz TW.** 2002. Murine cytomegalovirus (CMV) M33 and human CMV US28 receptors exhibit similar constitutive signaling activities. J. Virol. **76**:8161–8168.
25. **Reeves MB, Breidenstein A, Compton T.** 2012. Human cytomegalovirus activation of ERK and myeloid cell leukemia-1 protein correlates with survival of latently infected cells. Proc. Natl. Acad. Sci. U. S. A. **109**:588–593.
26. **Reeves MB, Compton T.** 2011. Inhibition of inflammatory interleukin-6 activity via extracellular signal-regulated kinase-mitogen-activated protein kinase signaling antagonizes human cytomegalovirus reactivation from dendritic cells. J. Virol. **85**:12750–12758.
27. **Kledal TN, Rosenkilde MM, Schwartz TW.** 1998. Selective recognition of the membrane-bound CX3C chemokine, fractalkine, by the human cytomegalovirus-encoded broad-spectrum receptor US28. FEBS Lett. **441**:209–214.
28. **Tschische P, Moser E, Thompson D, Vischer HF, Parzmair GP, Pommer V, Platzer W, Schwarzbraun T, Schaider H, Smit MJ, Martini L, Whistler JL, Waldhoer M.** 2010. The G protein-coupled receptor associated sorting protein GASP-1 regulates the signaling and trafficking of the viral chemokine receptor US28. Traffic **11**:660–674.